Bioactive Materials 9 (2022) 590–601

Contents lists available at ScienceDirect

Bioactive Materials

journal homepage: www.sciencedirect.com/journal/bioactive-materials

Ionizable lipid-assisted efficient hepatic delivery of gene editing elements for oncotherapy

Chunhui Li [a,1], Tongren Yang [a,1], Yuhua Weng [a,1], Mengjie Zhang [a], Deyao Zhao [a,b], Shuai Guo [a], Bo Hu [a], Wanxuan Shao [a], Xiaoxia Wang [c], Abid Hussain [a,d], Xing-Jie Liang [d], Yuanyu Huang [a,e,*]

[a] School of Life Science, Advanced Research Institute of Multidisciplinary Science, Institute of Engineering Medicine, Key Laboratory of Molecular Medicine and Biotherapy, Beijing Institute of Technology, Beijing, 100081, China
[b] Department of Radiation Oncology, The First Affiliated Hospital of Zhengzhou University, Erqi, Zhengzhou, 450000, China
[c] Institute of Molecular Medicine, College of Future Technology, Peking University, Beijing, 100871, China
[d] Chinese Academy of Sciences (CAS) Key Laboratory for Biomedical Effects of Nanomaterials and Nanosafety, CAS Center for Excellence in Nanoscience, National Center for Nanoscience and Technology of China, Beijing, 100190, China
[e] School of Materials and the Environment, Beijing Institute of Technology, Zhuhai, 519085, China

ARTICLE INFO

Keywords:
CRISPR/Cas
Gene editing
Lipid nanoparticle
PLK1
Cancer therapy

ABSTRACT

CRISPR/Cas9-based gene editing has emerged as a powerful biotechnological tool, that relies on Cas9 protein and single guided RNA (sgRNA) to edit target DNA. However, the lack of safe and efficient delivery carrier is one of the crucial factors restricting its clinical transformation. Here, we report an ionizable lipid nanoparticle (iLP181, p*Ka* = 6.43) based on iLY1809 lipid enabling robust gene editing *in vitro* and *in vivo*. The iLP181 effectively encapsulate psgPLK1, the best-performing plasmid expressing for both Cas9 protein and sgRNA targeting Polo-like kinase 1 (PLK1). The iLP181/psgPLK1 nanoformulation showed uniformity in size, regular nanostructure and nearly neutral zeta potential at pH 7.4. The nanoformulation effectively triggered editing of PLK1 gene with more than 30% efficiency in HepG2-Luc cells. iLP181/psgPLK1 significantly accumulated in the tumor for more than 5 days after a single intravenous injection. In addition, it also achieved excellent tumor growth suppression compared to other nucleic acid modalities such as siRNA, without inducing adverse effects to the main organs including the liver and kidneys. This study not only provides a clinically-applicable lipid nanocarrier for delivering CRISPR/Cas system (even other bioactive molecules), but also constitutes a potential cancer treatment regimen base on DNA editing of oncogenes.

1. Introduction

The development of CRISPR/Cas gene editing technology has entered in a promising era, offering new treatments for diseases that are currently incurable. It has been applied to treat cancer [1], blister skin disease [2], Huntington's disease [3], sickle cell disease (SCD) [4], HIV-1 infection [5], and to establish specific animal model carrying a modified genome [6], etc. It can also be used to detect certain nucleic acid molecules, facilitating disease diagnosis, pathogenic microorganism analysis and environmental monitoring [7,8]. To some extent, the emergence of CRISPR/Cas reflects the significant advances of human gene editing technology, and provides an effective and powerful platform to further understand gene functions, underlying biological or pathological mechanisms of various disease, and ultimately development of novel treatment regimens.

In order to transport CRISPR/Cas system into cells, various delivery technologies are used, such as electroporation, virus or non-viral carriers [9]. Viral carriers such as adeno-associated virus (AAV) and lentiviral vectors are frequently used to confer long-lasting effects, which helped in motivating the recent surge of successful gene therapies [10,11]. Two gene therapeutics based on AAV vectors, Luxturna and Zolgensma, have been approved by the U.S. Food and Drug Administration (FDA) in 2017

Peer review under responsibility of KeAi Communications Co., Ltd.
* Corresponding author. School of Life Science, Advanced Research Institute of Multidisciplinary Science, Institute of Engineering Medicine, Key Laboratory of Molecular Medicine and Biotherapy, Beijing Institute of Technology, Beijing, 100081, China.
E-mail address: yyhuang@bit.edu.cn (Y. Huang).
[1] These authors contributed equally to this work.

https://doi.org/10.1016/j.bioactmat.2021.05.051
Received 24 January 2021; Received in revised form 27 May 2021; Accepted 28 May 2021
Available online 25 June 2021

and 2019, respectively. Another therapeutic for the treatment of hemophilia A is expected to receive the FDA approval in 2021 [12]. However, safety concerns regarding AAV vectors have simmered for nearly 20 years. It was reported that newborn mice developed liver cancer after they were injected with a high dose of AAV vectors [13]. In 2018, James Wilson reported that a high dose of AAV vectors induced systemic and sensory neuron toxicities in juvenile nonhuman primates [14]. Recently, a study conducted on hemophilia dogs treated with AAV showed that the vector could insert payload into the host's genome, close to genes that control cell growth. Therefore, the scientific researchers are concerning that, it is only a matter of time before such insertions causes cancers [15]. In addition, the use of AAV to deliver Cas9 mRNA may also causes sustained Cas9 protein expression, anti-Cas9 immune response and off-target editing. There is currently a lack of *in vivo* evidence for the biomedical efficacy of lentiviral vector-facilitated Cas9 delivery.

Comparatively, non-viral carriers represent a safe and efficacious approach that allows long-term administration [11]. Among the available diverse carriers, lipid nanoparticles (LNPs) are the most clinically-advanced as compared to other available options [16–21]. For example, Onpattro®, the siRNA-loaded LNP formulation, has been approved by the US FDA for the treatment of transthyretin mediated amyloidosis. Moreover, the three recently mRNA-based COVID-19 vaccines (mRNA-1273, BNT162b2, CVnCoV) are all LNP formulations [22,23], and two of them (mRNA-1273 and BNT162b2) have been authorized the emergency use in December 2020 for the prevention of COVID-19. LNP is also the most potent delivery system for CRISPR/Cas and has been employed in delivering gene editing payloads to the cancer cells [1], hepatocytes [24–27], the lung [24] and the brain [28].

In addition, ionizable lipid can be protonated at acidic (endosomal) environment, interact with endosomal membrane's anionic lipids such as phosphatidylserine, facilitating membrane fusion, membrane disruption and endosomal escape [16,29], thus, highlighting its overwhelming advantages for nucleic acid delivery. Herein, we developed a novel ionizable LNP (iLNP), called iLP181, to evaluate its performances in delivering CRISPR/Cas system (Scheme 1). We constructed a plasmid containing the expression frame of Cas9 protein and sgRNA targeting PLK1 (polo-like kinase 1) gene, termed as Cas9-sgPLK1 plasmid or psgPLK1. The physicochemical properties of iLP181/psgPLK1 including the p*K*a value, size, morphology and zeta potential were characterized. The *in vitro* gene editing, intracellular delivery mechanism and *in vivo* biodistribution were explored. Finally, the therapeutic effects and toxicity of iLP181/psgPLK1 formulation on tumor-bearing mice were carefully evaluated.

2. Materials and methods

2.1. Materials

Cell culture reagents such as the Fetal bovine serum (FBS), trypsin, streptomycin-penicillin, Dulbecco's modified Eagle's medium (DMEM), Opti-MEM, Lipofectamine 2000 were purchased from Thermo Fisher. RNA*later*® and TRIzol® were purchased from Sigma-Aldrich (St Louis, MO). Luciferase substrate was purchased from Promega Co.Ltd (Madison, USA). PCR Mix and RT-PCR Mix were purchased from YEASEN Co. (Shanghai, China). The DMG-PEG_{2000} ((R)-2,3-bis(octadecyloxy)propyl-1-(methoxy polyethylene glycol 2000) carbamate) and DSPC (1,2-Dioctadecanoyl-*sn*-glycero-3-phophocholine) were purchased from Avanti Polar Lipids, Inc (Alabama, USA). The siPLK1, cholesterol and iLY1809 were provided by Suzhou Ribo Life Science Co. Ltd. (Suzhou, China). All the primers were provided by BioSune Co. (Shanghai, China).

2.2. Plasmid construction and preparation

Four sgRNAs targeting PLK1 gene were designed by using the online CRISPR design tool (http://crispr.mit.edu/). First, the expression cassette of sgPLK1 within sgRNAs lenti Guide-Puro was amplified by polymerase chain reaction (PCR) and cloned into the Bbs 1 restriction sites of PX458 plasmid. Then, the constructed Cas9-sgPLK1 plasmid (psgPLK1) was transfected into *E. coli* DH5α and cultivated at 37 °C in 400 mL LB broth (without ampicillin) for 4 h. Next, the *E. coli* DH5α solution was concentrated and streaked on solid LB culture (containing ampicillin) and incubated at 37 °C for 24 h. In the following days, the single colony of *E. coli* was added to LB culture (containing ampicillin) and was incubated for another 16 h at 37 °C. After cultivation, the *E. coli* was collected and the modified Cas9-sgPLK1 plasmid (psgPLK1) was purified with Endo Free Plasmid kits (TIANGEN).

2.3. Preparation and characterization of iLP181/psgPLK1 formulation

The iLP181/psgPLK1 formulation is prepared according to previous reports with some modification [16,17,30]. Briefly, the lipids containing cholesterol, DSPC, iLY1809 and DMG-PEG_{2000} were dissolved in ethanol solution and were added into sodium acetate solution to obtain the

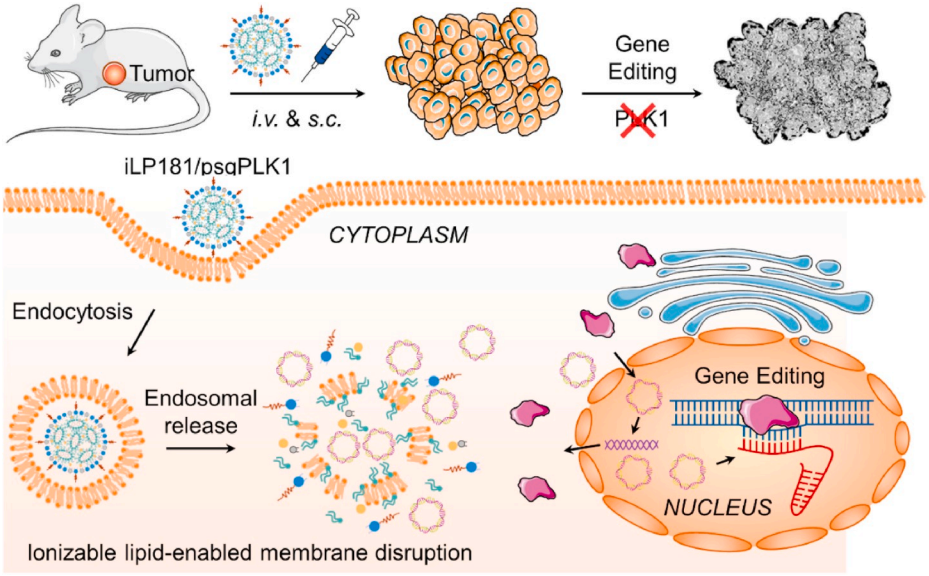

Scheme 1. Illustration of ionizable lipid nanoparticle (iLP181)-delivered CRISPR/Cas9 elements and the process of intracellular trafficking and gene editing.

pre-liposomes. Then the aqueous plasmid solution (300 ng/μL) was mixed with pre-liposomes at a volume ratio of 1:1. Subsequently, the mixture was incubated at 50 °C for 10–20 min, and dialyzed against PBS buffer to remove the organic phase. The final iLP181/psgPLK1 liposome formulation were used as prepared or kept at 4 °C for less than 3 months. The size, polydispersity index (PDI) and zeta potential of LNPs were determined by the Dynamic Light Scattering (DLS) equipment (Malvern, Zetasizer Nano ZS). The morphology was observed by transmission electron microscopy (TEM) (Hitachi, HT7700).

2.4. pKa determination

A fluorescent probe of 2-(*p*-toluidino)-6-napthalene sulfonic acid (TNS) was used to determine the p*K*a value of iLP181 formulation. First, iLP181 (10 mM) solution was prepared in PBS. Then a series of iLP181 solutions with a pH range of 3.00–10.00 were prepared, containing 1 μM TNS, 10 mM ammonium acetate, 10 mM 4-morpholineethanesulfonic acid (MES), 10 mM HEPES and 130 mM NaCl. The fluorescence intensity of each solution was measured with a spectrophotometer at the excitation wavelength of 321 nm and emission wavelength of 445 nm. The sigmoidal best fit analysis was performed to analyze the fluorescence data. The p*K*a value was calculated and defined as the pH giving rise to the semi-maximal fluorescence intensity [29].

2.5. Cell culture

HEK293A, human embryonic kidney cell line, and HepG2-Luc, human hepatocellular carcinoma cell line with stable luciferase expression, were cultured with DMEM containing 10% FBS, 100 IU/mL penicillin, and 100 g/mL streptomycin at 37 °C in a humidified atmosphere with 5% CO_2.

2.6. Plasmid validation using fluorescence microscopy

Because the expression frame of green fluorescence protein (GFP) was inserted to the backbone of the commercial PX458 plasmid, we validated the function of PX458 empty plasmid (PX458-E) and the freshly-constructed plasmid containing the expression frames of Cas9 and sgPLK1 (psgPLK1) with fluorescence microscopy. The HEK293A cells were seeded in 6-well plates with 2×10^5 cells per well and cultured overnight with complete medium. Then the cells were transfected with 1.6 μg PX458-E (600 ng/μL) or psgPLK1 (600 ng/μL) using Lipofectamine 2000 (Lipo2000) and cultured in Opti-MEM for 4 h followed by culturing in complete medium for another 20 h or 44 h. Cells transfected with the 1.6 μg siRNA (600 ng/μL) targeting PLK1 gene and cells without transfection were included as controls. After the cells were cultured for 24 h and 48 h, the GFP fluorescence was observed under a fluorescence microscope. Meanwhile, the GFP fluorescence intensity was quantified using Image J software.

To validate the delivery efficiency of the LNP, the HEK293A cells were transfected with iLP181/PX458-E and iLP181/psgPLK1 LNPs using the same transfection procedure as mentioned above. Cells without transfection or transfected with Lipo2000-formulated psgPLK1 were used as controls. When the cells were transfected for 24 h, the GFP expression and cellular location were observed using confocal laser microscopy (Nikon, Japan).

2.7. Screening of sgRNA sequence

HEK293A cells were plated into 6 well-plates (2×10^5 cells per well), and transfected with four iLP181/psgPLK1 LNPs with different sgPLK1 sequences in opti-MEM for 4 h using Lipo2000 and then were cultured in complete medium for another 20 h. Each well was added with iLP181/psgPLK1 LNPs containing 1.6 μg plasmid (600 ng/μL), and siRNA targeting PLK1 (siPLK1) was included as a control. Total RNA was extracted using TRIzol reagent. After the reverse transcription, the real time PCR reaction was run on QuantStudio 3&5 PCR system (Applied Biosystems, Thermo Fisher) using the SYBR Green PCR Master Mix. The GAPDH gene was used as an internal reference. The sequence of siPLK1 and primers used in PCR were shown in Table S1.

Long-term evaluation of the PLK1 mRNA knockdown efficiency was also performed in HepG2-Luc cells. Cells were transfected with iLP181 or Lipo2000-formulated psgPLK1 and PX458-E LNPs in complete medium. The PLK1 mRNA expression was evaluated using real time PCR after cells were transfected for 3 days. In addition, other groups of cells were also transfected with iLP181 or Lipo2000-formulated psgPLK1 and PX458-E LNPs. Three days later, cells were digested and half of cells were seeded. These cells were transfected for a second time. Four days later (day 7), the PLK1 mRNA expression was evaluated.

2.8. MTT assay

The HepG2-Luc cells were seeded in 96-well plates with 1×10^4 cells per well and were cultured overnight with complete medium. Then, the cells were transfected with iLP181-formulated psgPLK1, siPLK1 and PX458-E LNPs according to the same procedure as described above. At 24 h post-transfection, 100 μL MTT (0.2 mg/mL in DMEM) was added to each well instead of the complete medium and were cultured for 4 h at 37 °C. Subsequently, the medium containing MTT was removed. Then 50 μL DMSO was added into each well and incubated for 15 min. Lastly, the cell viability is calculated as follows:

$$\text{Cell viability}(\%) = \frac{OD_{540(Sample)} - OD_{650(Sample)}}{OD_{540(Mock)} - OD_{650(Mock)}} \times 100$$

OD_{540} stands for the absorbance of each well at 540 nm, and OD_{650} stands for the absorbance at 650 nm.

2.9. Stability evaluation

iLP181/psgPLK1 LNPs were incubated with PBS or 10% human serum (HS) at 4 °C for 14 days. The hydrodynamic diameters and zeta potentials of LNPs were recorded at 1 d, 3 d, 5 d, 7 d, 10 d, and 14 d by using dynamic light scattering (DLS) equipment (Malvern Instruments, UK).

2.10. Cellular uptake mechanism

The HepG2-Luc cells were seeded in 6-well plates with 2×10^5 cells per well and were cultured overnight with complete medium. The ApoE protein was incubated with iLP181/Cy5-labelled nucleic acid (iLP181/Cy5-NA) for 5 min at 37 °C. Then, the cells were transfected with iLP181/Cy5-NA or iLP181/Cy5-NA/ApoE mixture and cultured with Opti-MEM (serum-free medium) or DMEM (complete medium) for 4 h. After transfection, cells were washed by PBS for 3 times, stained by lysotracker Green DNA-26 and Hoechst 33342 for 15 min, and observed under a confocal laser scanning microscope (CLSM). Meanwhile, another parallel test was conducted for the flow cytometry analysis (BD, USA).

2.11. Endosomal escape efficiency

The HepG2-Luc cells were seeded in 6-well plates with 2×10^5 cells per well and were cultured overnight with complete medium. Before transfection, cells were treated with chloroquine (50 μM) and bafomycin A1 (200 nM) for 1 h. Then, cells pre-treated with chloroquine were transfected with iLP181/Cy5-NA and chloroquine, and cells pre-treated with bafomycin A1 were transfected with iLP181/Cy5-NA only. All groups of cells were transfected for 1, 3, 5, 8 or 10 h in DMEM complete medium. After transfection, cells were stained with Hoechst 33342 and lysotracker green DNA-26 and were examined by CLSM.

2.12. Animals

All animals were purchased from SPF (Beijing) biotechnology co., LTD. and maintained in Laboratory Animal Center. All the animals associated experimental procedures were performed in accordance with the principles of the Institutional Animal Care and Use Committee (IACUC) of Beijing Institute of Technology.

2.13. In vivo biodistribution

The 6–8 weeks old, weighing 18–22 g C57BL/6 mice were used for *in vivo* biodistribution study. The iLP181-formulated Cy5-nucleic acid (iLP181/Cy5-NA) or red fluorescent protein (RFP)-expressed plasmid (iLP181/plasmid) were prepared according to aforementioned protocol and were injected into mice via tail vein at the dose of 1 mg/kg. The concentration of Cy5-NA and RFP-expressed plasmid all are 600 ng/μL. The whole-body Cy5 expression was assessed at 1 h, 3 h, 6 h, 12 h and 24 h post injection using an *in vivo* imaging system (PerkinElmer, IVIS Lumina LT). At 6 h, 12 h and 24 h time point, one animal from each group was sacrificed and their main organs were collected and re-examined by *in vivo* imaging system. The mean fluorescence intensities (MFIs) of the tumors from the living animals and the isolated organs from sacrificed animals were quantitatively analyzed.

Furthermore, the whole-body RFP expression was also assessed at 2 d, 3 d and 5 d post injection. And at each time point, one animal from each group was sacrificed and their main organs were collected and re-examined by *in vivo* imaging system. The MFIs of the tumors and the organs from sacrificed animal were quantitatively analyzed, too.

2.14. Antitumor activity in vivo

HepG2-Luc cells (5×10^6 cells) were injected subcutaneously into the flanks of BALB/c nude mouse. When the volume of tumor reached 50 mm^3, the tumor-bearing mice were randomly divided into different groups, and were treated with PBS, iLP181/PX458-E, iLP181/siPLK1, iLP181/psgPLK1 by intratumoral injection, respectively. The mice were injected every 2–4 days at a dose of 0.5 mg/kg (for siRNA or plasmid) for 8 times. Body weights were monitored during the entire experiment and tumor volumes were recorded by a caliper. The tumor volumes were calculated as the formula: $V = L \times W^2 \times 1/2$, where V is volume, L is the length and W is the diameters of tumor. The PLK1 mRNA expression in tumor tissues were evaluated by RT-PCR method and the H&E staining of tumor sections were also conducted at the end of treatment.

2.15. Safety evaluation

In order to evaluate the *in vivo* toxicity of LNPs, different formulations including PBS, iLP181/siPLK1, iLP181/psgPLK1 and iLP181/PX458-E were intratumorally injected into the BALB/c nude mice every 2–4 days at a dose of 0.5 mg/kg (for siRNA or plasmid). Animal blood was drawn retro-orbitally and serum was isolated 21 days after drug administration. Serum specimens were prepared and the major blood biochemistry parameters including TBIL (Total Bilirubin), ALT (alanine transaminase), CREA (creatinine), AST (aspartate transaminase), TRIG (triacylglycerol) and UREA were examined. For histological examination, main organs including the liver, heart, lung, spleen, and kidney were collected at the end of experiment. Organ tissues were fixed with 4% paraformaldehyde, embedded in paraffin, and followed by sectioning and staining with H&E.

2.16. The statistical analysis

All data in the manuscript were expressed as mean ± SD, and differences between groups were considered significant with $P < 0.05$. One-way ANOVA analysis (GraphPad Software, La Jolla, CA, USA) was used to conduct statistical analysis for the comparison between two groups and comparison between multiple groups. Statistical differences were defined as $^*P < 0.05$ and $^{**}P < 0.01$.

3. Results and discussion

3.1. Construction of Cas9-sgPLK1 plasmid (psgPLK1)

PLK1 (polo-like kinase 1) is a serine/threonine kinase, that is highly expressed during the G2 phase of the cell cycle, where it control the metaphase-to-anaphase transition and mitotic exit [31]. It is often overexpressed in many tumor cells [32,33]. Knockout or knockdown of PLK1 gene by gene editing or other technologies is a promising approach for cancer treatment [1,34–37]. Before the construction of CRISPR/Cas9 plasmid, we designed four single chain sgRNA sequences targeting the PLK1 gene using an online design tool (http://crispr.mit.edu), and prepared double stranded sgRNAs by gradient annealing method. We then modified the commercial PX458 plasmid (PX458-E) by inserting sgRNA sequences into the sgRNA scaffold using T4 DNA ligase (Fig. S1). The modified plasmids were expanded by transfection and cultivation of *E coli*. The sequencing results demonstrated that there are no mismatch base pairs, which verified that the recombinant Cas9-sgPLK1 plasmid (psgPLK1) was successfully constructed (Fig. S1).

3.2. Preparation and characterization of iLP181 LNPs

To date, several ionizable lipids have been successfully developed for the delivery of RNAs and DNAs, such as Dlin-MC3-DMA and C12-200. Conventionally, an ionizable lipid consists of hydrophilic amino head and hydrophobic alkyl chain tails. Lipid containing ionizable amines has been reported to deliver small RNAs more effectively *in vivo* than non-ionized lipids which contain permanently charged quaternary amine moieties in their hydrophilic head group. Excellent intracellular delivery relies on an optimal balance of ionized amines to facilitate the binding and release of nucleic acids by LNPs. p*K*a value is an important molecular characteristic of ionizable lipids, and lipids with pKa value between 6.2 and 6.5 showed better siRNA delivery *in vivo*. With such a sharp p*K*a, ionizable LNPs have minimum charge in neutral physiological environment to maximize hepatocyte uptake by ApoE-mediated endocytosis and maximum positive charge in acidic endosomal compartment to promote membrane disruption. As a result, lipids with p*K*a value between 6.2 and 6.5 achieve a balance between the two opposing delivery requirements, improving the resulting functionality. The p*K*a of clinically-applied Dlin-MC3-DMA was 6.44, and the ED_{50} (median effective dose for FVII gene silencing in female C57BL/6 mice by i.v. administration) of LNPs prepared based on Dlin-MC3-DMA and C12-200 is 0.03 mg/kg (before composition optimization) or 0.005 mg/kg (after composition optimization) [38], and 0.02 mg/kg [39], respectively, which were two of the lipids with the best delivery efficiency reported at present. In addition to p*K*a, appropriate hydrophobic tail numbers, length and lipid chain unsaturation also served as important considerations for lipid design. Based on these lipid design principles, we synthesized and screened an ionizable lipid, named iLY1809. The chemical structures of iLY1809, DSPC, DMG-PEG_{2000} and cholesterol were shown in Fig. S2.

The iLY1809 based LNPs (iLP181) containing various lipids were easily prepared by pumping the lipid solution (the organic phase) into the citrate buffer to form classic bilayer-structured vesicles (Fig. 1A). The CRISPR/Cas9 plasmids were then encapsulated into the LNPs through an additional incubation step with iLP181. This incubation step is essential for reassembling of LNPs and stabilizing the system. The lipid iLY1809 employed in this study is a proprietary ionizable lipid, which exhibits positive charges and entrap nucleic acids at acidic pH but becomes neutral charge at physiological pH. The PEG lipid affords a diffusible outer PEG layer to increase the half-life of LNPs in the bloodstream [40]. The DSPC influence the morphology and size of the nanoparticles, thereby affecting the delivery efficiency [41]. The last

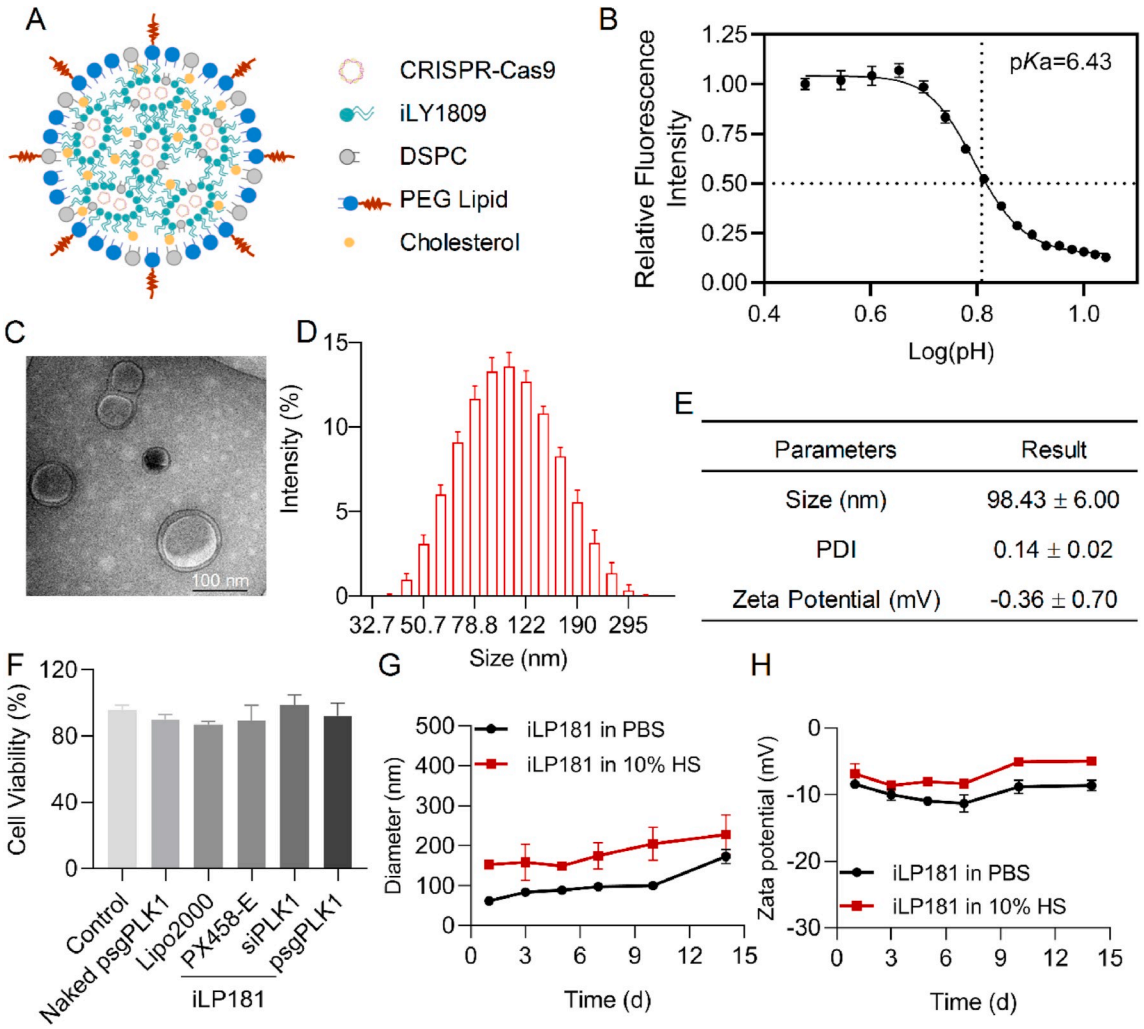

Fig. 1. Physicochemical characteristics of iLP181 LNPs. (A) The schematic diagram of LNPs. (B) The p*Ka* value of iLP181 formulation determined via TNS assay. (C) The morphology of LNPs was visualized by TEM. (D and E) The physicochemical parameters and size distribution of the formulation. (F) The cell viability was measured by MTT assay. (G and H) The stability of iLP181 LNPs was evaluated in body fluid-mimicking system for two weeks. HS, human serum.

component cholesterol is the most common lipid used in preparation of LNPs, which helps to stabilize the LNP [41,42]. The pKa value of iLP181 formulation determined by TNS assay was approximately 6.43 (Fig. 1B), which was in line with our designing concept and met the requirements of ionizable lipid nanoparticle enabling efficient endosomal escape of the nucleic acid payloads in cells [38,43]. In addition, the formulated iLP181/CRISPR LNPs showed uniform spherical shapes with clear bilayer membranes (Fig. 1C). The size was approximately 100 nm (Fig. 1C, D and 1E). The polydispersity index (PDI) was lower than 0.2, indicating a narrow distribution of particle size (Fig. 1E). The zeta potential was close to neutral at physiological pH. More than 85% cell viability was observed in the iLP181 formulation-treated cells, indicating the ideal biocompatibility of iLP 181 LNPs *in vitro* (Fig. 1F).

Furthermore, The stability of iLP181/psgPLK1 LNPs was measured in body fluid-mimicking system. The size and zeta potential of LNPs were stable and uniform after they were incubated in PBS or in 10% human serum for two weeks, verifying the outstanding stability and relative safe character of iLP181 LNPs (Fig. 1G and H).

3.3. *In vitro gene editing efficiency of iLP181/psgPLK1 LNPs*

To validate the gene editing efficiency, we transfected psgPLK1 to the HEK293A cells using Lipo2000. The expression of GFP, a tag protein in PX458 plasmid, was observed by fluorescence microscope at 24 h and 48 h post transfection, respectively (Figs. S3A and S3B). It was illustrated that both PX458-E and psgPLK1 effectively expressed GFP in HEK293A cells. In addition, the delivery efficiency of iLP181 LNPs in cells were also evaluated by laser confocal microscopy. As shown in Figs. S3C and 3D, the GFP expression pattern was the same with that shown in Figs. S3A and 3B. Therefore, the iLP181 displayed comparable intracellular delivery efficiency with Lipo2000 for CRISPR/Cas plasmid.

In addition, based on the self-designed series of sgRNA sequences targeting PLK1 gene, we also constructed a series of CRISPR/Cas9 plasmids and evaluated their gene editing efficiency in HEK293A cells using Lipo2000. It was shown that the sgPLK1-1 sequence exhibited the best activity and the gene editing efficiency reached 33% (Fig. 2A). We then formulated the psgPLK1 plasmid containing sgPLK1-1 sequence with iLP181 and detected the long-term mRNA knockdown performance in HepG2-Luc cells. Cells were transfected for 3 d and 7 d, respectively, and were collected to analyze the mRNA level. It was revealed that iLP181 mediated remarkable mRNA knockdown efficiency in HepG2-Luc cells, especially 32% knockout efficiency on 7 d, indicating that the plasmid-mediated gene editing effect was long-term (Fig. 2B).

It is reported that ionizable LNP (iLNPs) can deliver the payloads to hepatocytes via an active liver-targeting mechanism. When iLNPs are systemically administered, they may bind with apolipoprotein E (ApoE) in circulation, then interact with low-density lipoprotein receptor (LDLR), a highly-expressed protein on hepatocytes, and finally being

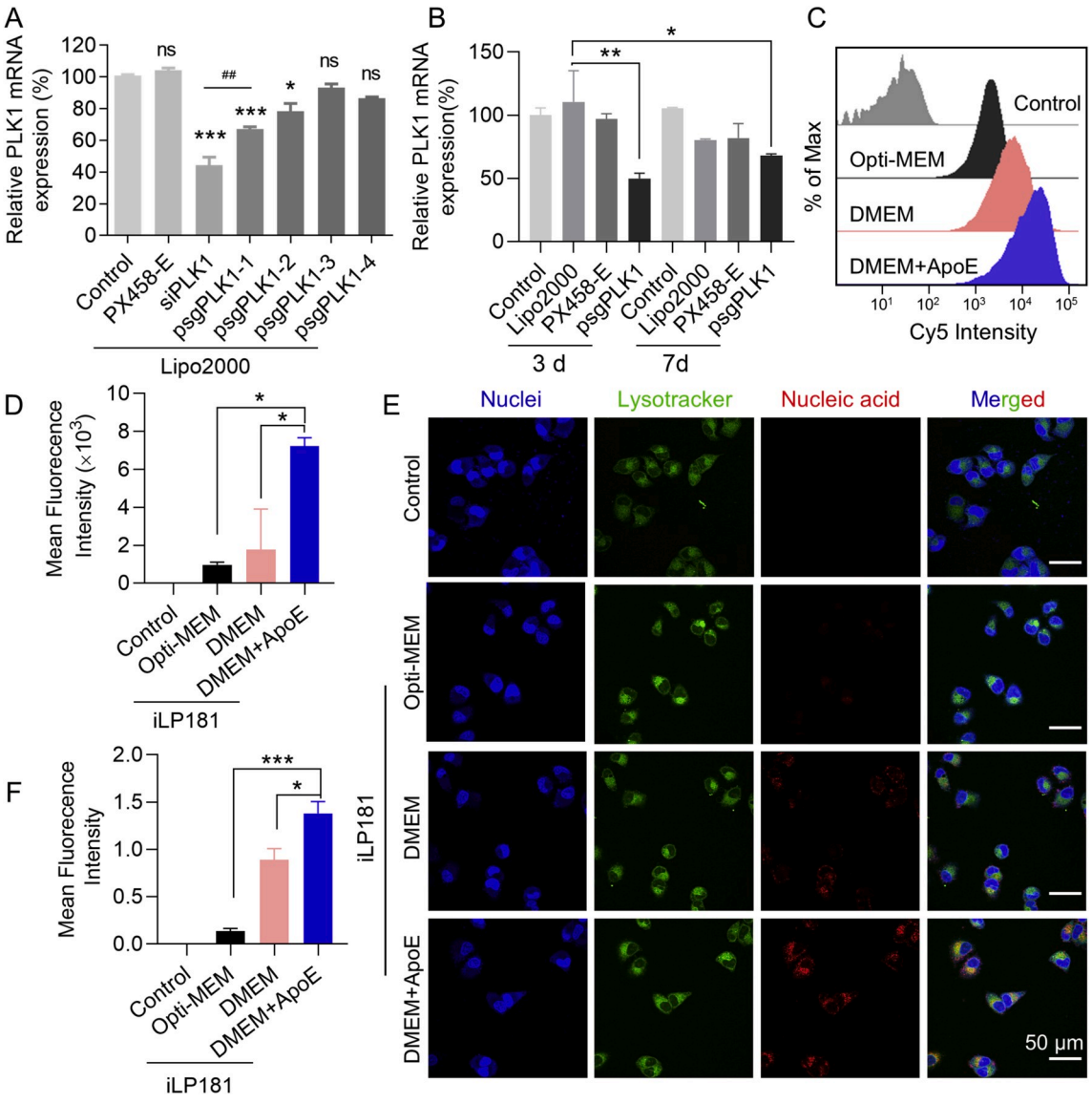

Fig. 2. Evaluation of iLP181/psgPLK1-mediated gene editing and endocytosis mechanism on cells. (A) sgRNA sequence selection. (B) Long-term evaluation of iLP181/psgPLK1-mediated gene editing in HepG2-Luc cells. (C–F) ApoE-dependent cellular uptake of iLP181 LNPs in HepG2-Luc cells. (C) Flow cytometry recorded internalization of iLP181 LNPs. (D) Quantitative analysis of (C) by using FlowJo 7.6.1 software. (E) Confocal laser scanning microscopy (CLSM) images of cells received various treatments. Scale bar, 50 μm. (F) Quantitative analysis of (E) by using Image J software. Opti-MEM and DMEM represented the cells transfected with iLP181/Cy5-NA in serum-free medium (Opti-MEM) or complete medium (DMEM), respectively. 'DMEM+ApoE' represented the cells treated with iLP181/Cy5-NA/ApoE mixture in complete medium. Cy5-NA, Cy5-labelled nucleic acid. $^{\#}$ represents comparison with Lipo2000/siPLK1, * represents the comparison with control in (A) or Lipo2000/psgPLK1 in (B). * or $^{\#}$, $P < 0.05$; ** or $^{\#\#}$, $P < 0.01$; *** or $^{\#\#\#}$, $P < 0.001$. "ns", no statistical difference.

internalized by hepatocytes via LDLR-mediated endocytosis [43,44]. In this study, the LDLR over-expressed HepG2-Luc cells were used to evaluate whether ApoE was an important factor for cellular uptake of iLNPs. As shown in Fig. 2C and D, it can be clearly found that when ApoE was added into the culture medium, the amounts of cellular uptake iLP181 LNPs were significant more than that without ApoE, demonstrating that the ApoE significantly boosted the cellular uptake of iLNPs. In addition, subcellular localization of the payload nucleic acids also verified that ApoE promoted the internalization of iLP181 LNPs (Fig. 2E and F).

3.4. The endosomal escape

Increasing evidences demonstrated that only 3.5% (even less than 1%) internalized nucleic acid can escape from endosome and be released into the cytosol to mediate gene silencing [45–48], necessitating the development of delivery vehicles with the ability of rapid endosomal escape. Hence, we conducted the experiments to explore the endosomal escape of iLP181 and compare the advantages between iLP181 and commercial transfection reagents Lipo2000. In Fig. S4A, the internalization and intracellular trafficking of iLP181/Cy5-lablled nucleic acids (iLP181/Cy5-NA) into HepG2-Luc cells were carefully investigated to elucidate the underlying mechanism. It was observed that, 1–3 h after transfection, the iLP181/Cy5-NA and Lipo2000/Cy5-NA entered the cells and were internalized by endosome or lysosomes (Figs. S4A, 4B, 4D, 4E). Variously, approximately 3–5 h after transfection, the iLP181/Cy5-NA escaped from the endosome/lysosome (Fig. S4C), while there was no significant escape from endosomes in the groups of Lipo2000 (Fig. S4F). The MFI of iLP181/Cy5-NA and Lipo2000/Cy5-NA increased with the extension time of transfection, indicating more and more nucleic acids accumulated in HepG2-Luc cells (Figs. S4B and 4E).

We further examined the internalization and subcellular localization

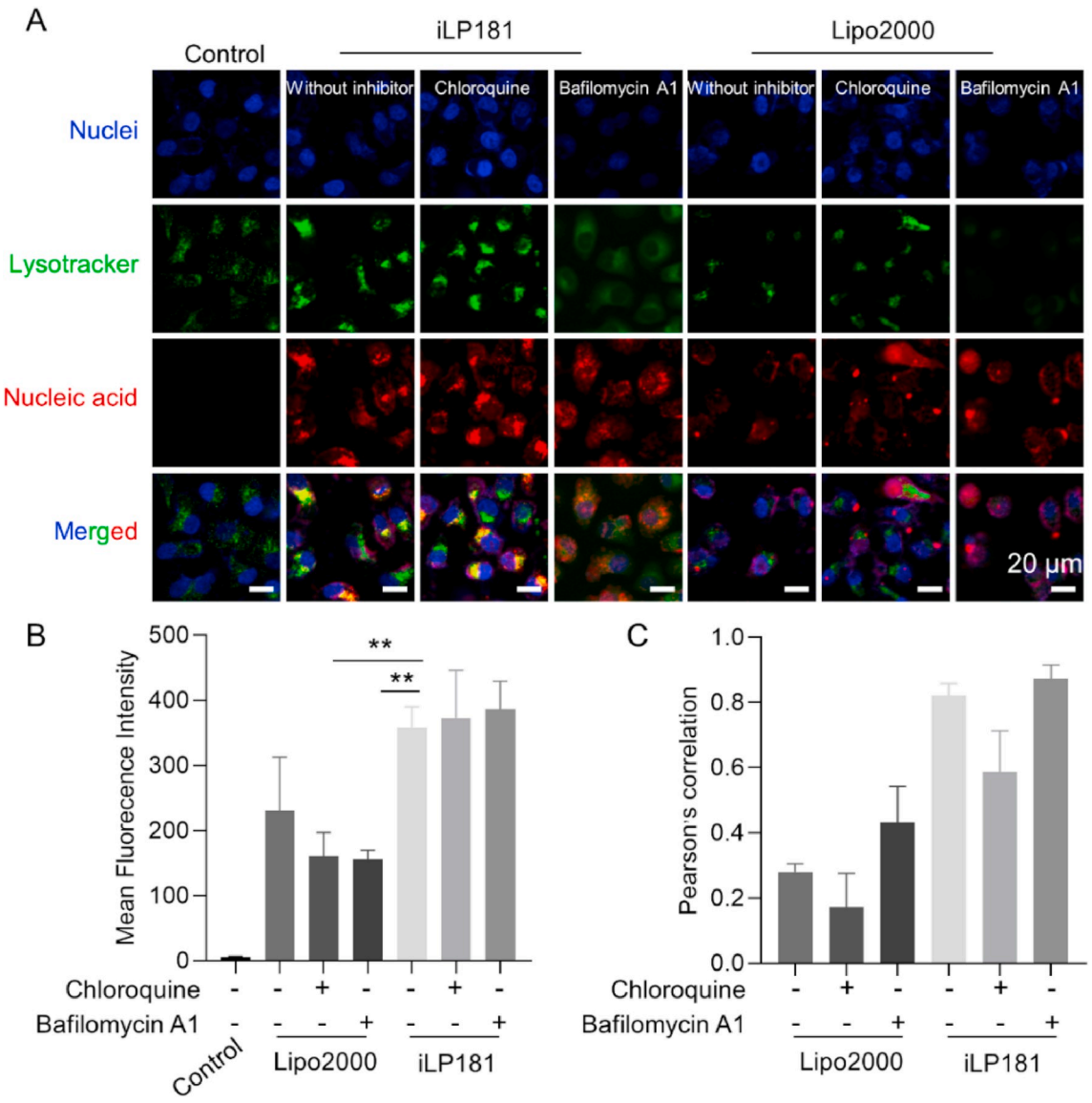

Fig. 3. Endosomal escaping of iLP181 on cells. (A) Subcellular localization of iLP181/Cy5-NA in HepG2-Luc cells observed with confocal laser scanning microscopy (CLSM). Scale bars, 20 μm. (B) Mean fluorescence intensities (MFIs) of Cy5-NA. (C) Colocalization ratio of Cy5-NA and Lysotracker Green-stained endosomes. The MFI and colocalization ratio were analyzed with Nikon NIS-Elements analysis software. *, $P < 0.05$; **, $P < 0.01$.

(Fig. 3A) in the presence of chloroquine (50 μM, a lysosomal disrupting agent) and bafilomycin A1(200 nM, a proton pump inhibitor that selectively inhibits vacuolar H+- ATPase) to evaluate whether the iLP181/nucleic acid induce effective transfection enhancement and whether iLP181 utilize lysosome/endosome for intracellular trafficking, respectively [49]. The transfection of iLP181 LNPs and Lipo2000 formulation was conducted in complete medium (DMEM) containing serum. The MFIs of iLP181 LNPs was significantly stronger than the group Lipo2000 (Fig. 3B). Meanwhile, the colocalization ratio between nucleic acid and lysosome/endosome was calculated and applied to evaluated the endosome escape efficiency. Addition of chloroquine to the cell led to a significant decrease in the colocalization ratio value of the iLP181 LNPs (~58.33%) and Lipo2000 formulation (~17.26%), whereas addition of bafilomycin A1 to the cell led to a significant increase in the colocalization ratio value of the LP181 LNPs (~87.00%) and Lipo2000 formulation (~43.32%) (Fig. 3C). The MFIs of the Lipo2000/Cy5-NA were generally weak, which results in a smaller colocalization value compared to the iLP181/nucleic acid complexes. The results showed that chloroquine slightly increased transfection of iLP181 LNPs and Lipo2000, while bafilomycin A1 decreased their transfection (Fig. 3C).

3.5. *In vivo* biodistribution

We then evaluated the biodistribution of iLP181 LNPs in tumor-bearing mice. The Cy5-NA and red fluorescent protein (RFP)-expressed plasmid were formulated with iLP181 to prepare uniform LNPs, which were administered via tail vein into C57BL/6 mice at a dose of 1 mg/kg (Fig. 4). The Cy5 and RFP fluorescence were assessed by an *in vivo* imaging system at different time points. As shown in Fig. 4A and B, the Cy5 fluorescence in group of naked Cy5-NA disappeared at 24 h post administration, whereas iLP181 LNPs exhibited significant strong fluorescence for at least 24 h in mice and mainly accumulated in the liver and tumor. The quantitative analysis of mean fluorescence intensities confirmed the above results (Fig. 4C-F). Furthermore, the expression of RFP was also detected. In Fig. 4G, it was found that the LNPs group had the strongest RFP fluorescence signal in tumors within the examined hours. It is extremely difficult for naked nucleic acids to accumulate in tumors. Moreover, the RFP fluorescence intensities in tumors did not significantly reduce within 5 d. This phenomenon was consistent with

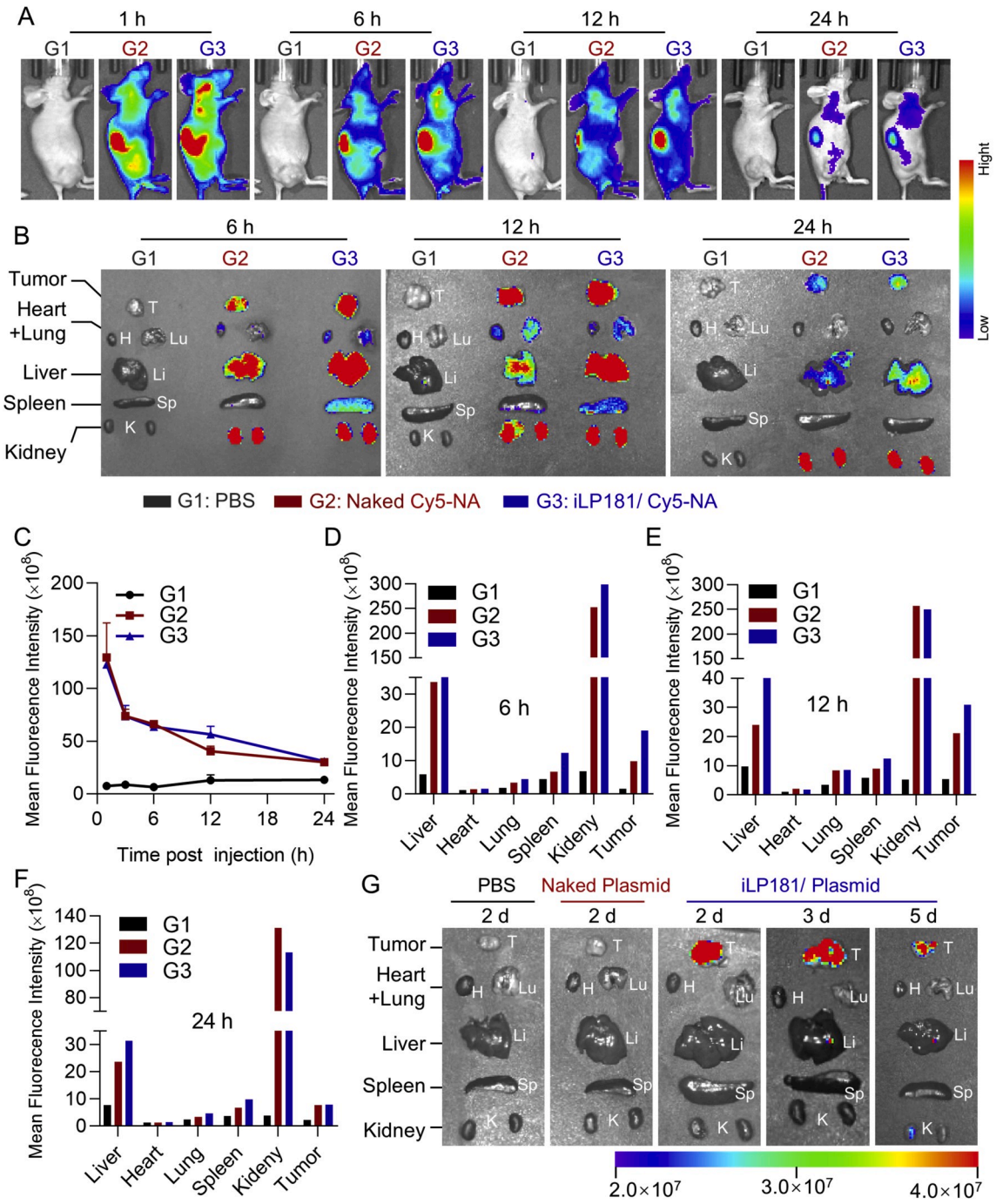

Fig. 4. *In vivo* biodistribution of iLP181/psgPLK1 LNPs. (A)The whole body and (B) isolated main organs were fluorescently examined using an *in vivo* imaging system at different times post administration. The mean fluorescence intensities (MFIs) of the tumors *in vivo* (C) and the isolated organs at (D) 6 h, (E) 12 h and (F) 24 h were quantitatively analyzed. (G) The isolated organs were imaged at 2 d, 3 d and 5 d post administration.

the fluorescence quantitative analysis of various organs (Fig. S5). These results suggested that iLP181 was an excellent systemic delivery system for CRISPR/Cas system.

3.6. Anti-tumor activity in vivo

PLK1 is considered a proto-oncogene involved in cell cycle regulation, neoplastic transformation and tumor suppressor p53 related pathways. Overexpression of PLK1 is a comment event in tumor cells. Liposomal siPLK1 formulation, TKM-080301, previously was investigated in phase II clinical trial for treating solid tumors [50]. Thus, anti-tumor effect of iLP181/psgPLK1 was assessed using a xenograft tumor-bearing murine model. The mice were given different formulations every other day, their tumor volume and weight were recorded (Fig. 5A). At the end of experiment, the expression of luciferase in tumors were detected by intraperitoneal injection of luciferase substrate. Compared with other groups, the luciferase activity in iLP181/psgPLK1-treated mice was significantly reduced, which should be attributed to the shrinkage of the tumor and decrease of cancer cell population induced by gene abolishment of PLK1 (Fig. 5B). In addition, the changes of tumor volume were recorded (Fig. 5C), indicating that the tumor growth rate of iLP181/psgPLK1 group was significantly slower than that of other groups. At the end of the experiment, tumors were isolated and the total RNA was extracted. It was observed that

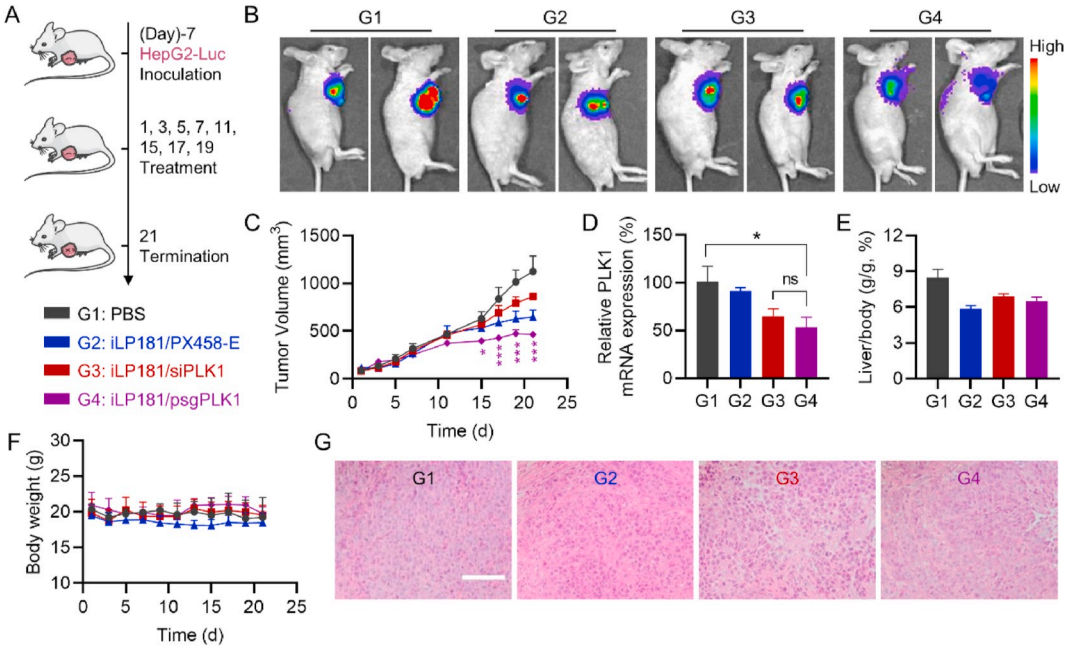

Fig. 5. *In vivo* anti-tumor efficacy of iLP181/psgPLK1 LNPs. (A) Scheme of tumor inoculation and intratumoral injection of PBS, iLP181/PX458-E, iLP181/siPLK1, and iLP181/psgPLK1 in HepG2-Luc tumor-bearing mice. Mice were injected 7 days post tumor inoculation (day 1). Injections were performed every 2–4 days for 8 times. (B) Bioilluminance imaging of animals at the end of experiment. (C) Tumor growth curves monitored throughout the experimental period. (D) PLK1 mRNA expression in the tumor tissues at the end of experiment. (E) Organ coefficient of the liver at the end of experiment. (F) Body weight recorded during the treatment course. (G) H&E staining of tumor sections prepared at the end of treatment. Scale bar, 50 μm. N = 6. * represents comparison with PBS, and *, $P < 0.05$; ***, $P < 0.001$. "ns", means no statistical difference.

PLK1 mRNA expression was obviously inhibited by iLP181/psgPLK1 (Fig. 5D), suggesting gene editing happened in this group. The iLP181/siPLK1 group showed comparable inhibition efficiency with respect to PLK1 mRNA, because no difference was observed between iLP181/psgPLK1 and iLP181/siPLK1. Moreover, no significant changes of body weight (Fig. 5E) and liver/body weight ratio (Fig. 5F) were recorded, which confirmed that iLP181 formulation did not trigger significant adverse effects in mice. The H&E staining of tumor sections further manifested that significant cell apoptosis and death occurred in animals treated with iLP181/psgPLK1 or iLP181/siPLK1 (Fig. 5G). These results illustrated that gene editing system of psgPLK1 was successfully delivered into the tumor cells by iLP181, and significant inhibition of tumor growth *in vivo* was achieved. Considering the PLK1 is a widely expressed and overexpressed oncogene, the iLP181/psgPLK1 can be applied to treat other tumors with high expression of PLK1 gene, such as lung cancer, breast cancer and so on.

3.7. In vivo safety evaluation of iLP181 LNPs

The hemolysis assay was applied to evaluate the iLP181 LNPs safety in blood circulation system (Fig. 6A). There was no hemolysis occurred in the groups of iLP181-formulated PX458-E, siPLK1 and psgPLK1 LNPs at pH7.4, whereas a little hemolysis appeared in these groups at pH5.5, reveled that iLP181 LNPs was safe enough in physiological circumstances, while effective endosome escape might occur in acid environment. Moreover, the *in vivo* toxicity of iLP181 formulations were further evaluated after the mice were treated with different LNPs for more than 20 days. The blood samples were collected for serum biochemical test and main organs were dissected for H&E staining at the end of the experiment. The functions of the liver and the kidney, two dominant distribution and elimination organs of iLP181 formulation, were well maintained as the serum biochemistry parameters all remained at the normal level (Fig. 6B). More importantly, compared with PBS group (Fig. 6C), iLP181/psgPLK1 did not cause any pathological damage to the main organs. Based on these observations, we concluded that iLP181 formulation was well tolerated by the animals, and it can be used for safe and effective delivery of CRISPR/Cas system *in vitro* as well as *in vivo*.

4. Conclusion

CRISPR/Cas technology has emerged as a powerful genome editing tool for biomedical applications. However, development of safe and efficient non-viral delivery technology for CRISPR/Cas system is urgently required and challenging. We here reported a proprietary ionizable lipid-based LNP, termed iLP181, and thoroughly evaluated its performance of delivering anti-cancer CRISPR/Cas9 system both *in vitro* and *in vivo*. Four plasmids containing the expression frame of Cas9 protein and sgRNA targeting PLK1 were designed and screened. One of them with the best activity (psgPLK1) was selected, and loaded with iLP181. Our study proved that iLP181/psgPLK1 was effectively internalized by hepatoma carcinoma cells by binding with ApoE. Long-term gene editing was achieved both *in vitro* and *in vivo*. Moreover, iLP181 LNPs exhibited robust endosomal escape in delivering nucleic acids compared with commercial Lipo2000, thus leading to significant tumor growth inhibition in tumor-bearing mice. In addition, proposed lipid formulation showed ideal *in vivo* safety profile. Therefore, this study provides a powerful non-viral delivery platform for CRISPR/Cas system, and a potential treatment regimen for gene editing-based cancer treatment.

CRediT authorship contribution statement

Chunhui Li: Investigation, Methodology, Formal analysis, Data curation, Writing – original draft. **Tongren Yang:** Investigation, Methodology, Formal analysis, Data curation. **Yuhua Weng:** Investigation, Formal analysis, Writing – review & editing, Funding acquisition. **Mengjie Zhang:** Investigation. **Deyao Zhao:** Investigation. **Shuai Guo:** Investigation. **Bo Hu:** Methodology. **Wanxuan Shao:** Investigation. **Xiaoxia Wang:** Formal analysis. **Abid Hussain:** Formal analysis. **Xing-Jie Liang:** Formal analysis. **Yuanyu Huang:** Conceptualization,

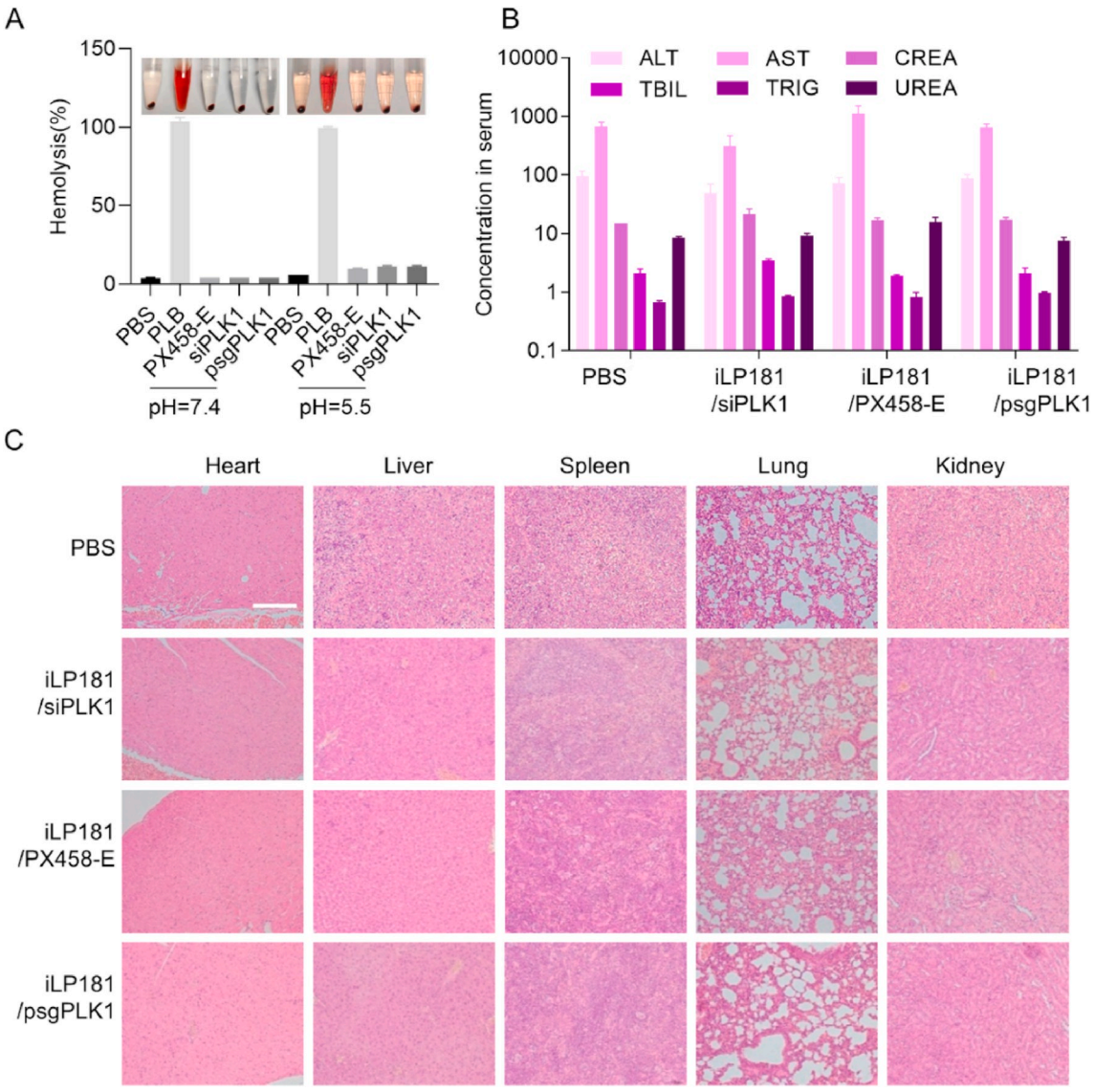

Fig. 6. *In vivo* safety evaluation of iLP181 formulations. Mice were treated with various iLP181 formulations via intravenously injection at a dose of 0.5 mg/kg (for siRNA or plasmid). (A) Hemolysis assay. (B) Examinations of serum biochemistry parameters. (C) H&E staining of the major organ sections. Scale bar, 100 μm.

Methodology, Formal analysis, Data curation, Writing – review & editing, Visualization, Supervision, Funding acquisition.

Declaration of competing interest

The authors declare no conflict of interest.

Acknowledgements

This work was supported by the Hu-Xiang Young Talent Program (2018RS3094), the Hunan Provincial Natural Science Foundation of China (2019JJ50196, 2018JJ1019), the Natural Science Foundation of Guangdong Province (2019A1515010776), the National Natural Science Foundation of China (31901053, 32001008, 31871003), the Beijing Nova Program from Beijing Municipal Science & Technology Commission (Z201100006820005), the Beijing-Tianjin-Hebei Basic Research Cooperation Project (19JCZDJC64100), the National Key R&D Program of China (2019YFE0133300), the Young Elite Scientist Sponsorship Program of Beijing Association for Science and Technology (2020–2022), and the Postdoctoral Science Foundation of China (2020M670169). We thank Biological & Medical Engineering Core Facilities (Beijing Institute of Technology) for providing advanced equipment.

Appendix A. Supplementary data

Supplementary data to this article can be found online at https://doi.org/10.1016/j.bioactmat.2021.05.051.

References

[1] D. Rosenblum, A. Gutkin, R. Kedmi, S. Ramishetti, N. Veiga, A.M. Jacobi, M. S. Schubert, D. Friedmann-Morvinski, Z.R. Cohen, M.A. Behlke, J. Lieberman, D. Peer, CRISPR-Cas9 genome editing using targeted lipid nanoparticles for cancer therapy, Sci Adv 6 (2020), eabc9450.

[2] S. Hainzl, P. Peking, T. Kocher, E.M. Murauer, F. Larcher, M. Del Rio, B. Duarte, M. Steiner, A. Klausegger, J.W. Bauer, J. Reichelt, U. Koller, COL7A1 editing via CRISPR/Cas9 in recessive dystrophic epidermolysis bullosa, Mol. Ther. 25 (2017) 2573–2584.

[3] X. Xu, Y. Tay, B. Sim, S.I. Yoon, Y. Huang, J. Ooi, K.H. Utami, A. Ziaei, B. Ng, C. Radulescu, D. Low, A.Y.J. Ng, M. Loh, B. Venkatesh, F. Ginhoux, G.J. Augustine, M.A. Pouladi, Reversal of phenotypic abnormalities by CRISPR/Cas9-Mediated

gene correction in Huntington disease patient-derived induced pluripotent stem cells, Stem Cell Reports 8 (2017) 619–633.
[4] J. Wen, W. Tao, S. Hao, Y. Zu, Cellular function reinstitution of offspring red blood cells cloned from the sickle cell disease patient blood post CRISPR genome editing, J. Hematol. Oncol. 10 (2017) 119.
[5] R. Kaminski, Y. Chen, J. Salkind, R. Bella, W.B. Young, P. Ferrante, J. Karn, T. Malcolm, W. Hu, K. Khalili, Negative feedback regulation of HIV-1 by gene editing strategy, Sci. Rep. 6 (2016) 31527.
[6] S. Chen, N.E. Sanjana, K. Zheng, O. Shalem, K. Lee, X. Shi, D.A. Scott, J. Song, J. Q. Pan, R. Weissleder, H. Lee, F. Zhang, P.A. Sharp, Genome-wide CRISPR screen in a mouse model of tumor growth and metastasis, Cell 160 (2015) 1246–1260.
[7] H. Khan, A. Khan, Y. Liu, S. Wang, S. Bibi, H. Xu, Y. Liu, S. Durrani, L. Jin, N. He, T. Xiong, CRISPR-Cas13a mediated nanosystem for attomolar detection of canine parvovirus type 2, Chin. Chem. Lett. 30 (2019) 2201–2204.
[8] J. Gong, L. Kan, X. Zhang, Y. He, J. Pan, L. Zhao, Q. Li, M. Liu, J. Tian, S. Lin, Z. Lu, L. Xue, C. Wang, G. Tang, An enhanced method for nucleic acid detection with CRISPR-Cas12a using phosphorothioate modified primers and optimized gold-nanopaticle strip, Bioact Mater. 6 (2021) 4580–4590.
[9] B. Hu, Y. Weng, X.H. Xia, X.J. Liang, Y. Huang, Clinical advances of siRNA therapeutics, J. Gene Med. 21 (2019), e3097.
[10] B. Hu, L. Zhong, Y. Weng, L. Peng, Y. Huang, Y. Zhao, X.J. Liang, Therapeutic siRNA: state of the art, Signal Transduct. Target. Ther. 5 (2020) 101.
[11] Y. Weng, H. Xiao, J. Zhang, X.J. Liang, Y. Huang, RNAi therapeutic and its innovative biotechnological evolution, Biotechnol. Adv. 37 (2019) 801–825.
[12] G.Q. Perrin, R.W. Herzog, D.M. Markusic, Update on clinical gene therapy for hemophilia, Blood 133 (2019) 407–414.
[13] M.A. Kay, C.S. Manno, M.V. Ragni, P.J. Larson, L.B. Couto, A. McClelland, B. Glader, A.J. Chew, S.J. Tai, R.W. Herzog, V. Arruda, F. Johnson, C. Scallan, E. Skarsgard, A.W. Flake, K.A. High, Evidence for gene transfer and expression of factor IX in haemophilia B patients treated with an AAV vector, Nat. Genet. 24 (2000) 257–261.
[14] C. Hinderer, N. Katz, E.L. Buza, C. Dyer, T. Goode, P. Bell, L.K. Richman, J. M. Wilson, Severe toxicity in nonhuman primates and piglets following high-dose intravenous administration of an adeno-associated virus vector expressing human SMN, Hum. Gene Ther. 29 (2018) 285–298.
[15] J. Kaiser, Virus used in gene therapies may pose cancer risk, dog study hints, Science (2020), https://doi.org/10.1126/science.aba7696.
[16] T. Yang, C. Li, X. Wang, D. Zhao, M. Zhang, H. Cao, Z. Liang, H. Xiao, X.J. Liang, Y. Weng, Y. Huang, Efficient hepatic delivery and protein expression enabled by optimized mRNA and ionizable lipid nanoparticle, Bioact Mater. 5 (2020) 1053–1061.
[17] S. Zheng, X. Wang, Y.H. Weng, X. Jin, J.L. Ji, L. Guo, B. Hu, N. Liu, Q. Cheng, J. Zhang, H. Bai, T. Yang, X.H. Xia, H.Y. Zhang, S. Gao, Y. Huang, siRNA knockdown of RRM2 effectively suppressed pancreatic tumor growth alone or synergistically with doxorubicin, Mol. Ther. Nucleic Acids 12 (2018) 805–816.
[18] J. Ye, Y. Yang, J. Jin, M. Ji, Y. Gao, Y. Feng, H. Wang, X. Chen, Y. Liu, Targeted delivery of chlorogenic acid by mannosylated liposomes to effectively promote the polarization of TAMs for the treatment of glioblastoma, Bioact Mater. 5 (2020) 694–708.
[19] Y. Zhou, A. Fang, F. Wang, H. Li, Q. Jin, L. Huang, C. Fu, J. Zeng, Z. Jin, X. Song, Core-shell lipid-polymer nanoparticles as a promising ocular drug delivery system to treat glaucoma, Chin. Chem. Lett. 31 (2020) 494–500.
[20] Y. Wang, F. Gao, X. Jiang, X. Zhao, Y. Wang, Q. Kuai, G. Nie, M. He, Y. Pan, W. Shi, S. Ren, Q. Yu, Co-delivery of gemcitabine and Mcl-1 SiRNA via cationic liposome-based system enhances the efficacy of chemotherapy in pancreatic cancer, J. Biomed. Nanotechnol. 15 (2019) 966–978.
[21] S. Yu, X. Bi, L. Yang, S. Wu, Y. Yu, B. Jiang, A. Zhang, K. Lan, S. Duan, Co-delivery of paclitaxel and PLK1-targeted siRNA using aptamer-functionalized cationic liposome for synergistic anti-breast cancer effects in vivo, J. Biomed. Nanotechnol. 15 (2019) 1135–1148.
[22] E.E. Walsh, R.W. Frenck Jr., A.R. Falsey, N. Kitchin, J. Absalon, A. Gurtman, S. Lockhart, K. Neuzil, M.J. Mulligan, R. Bailey, K.A. Swanson, P. Li, K. Koury, W. Kalina, D. Cooper, C. Fontes-Garfias, P.Y. Shi, Ö. Türeci, K.R. Tompkins, K. E. Lyke, V. Raabe, P.R. Dormitzer, K.U. Jansen, U. Şahin, W.C. Gruber, Safety and immunogenicity of two RNA-based covid-19 vaccine candidates, N. Engl. J. Med. 383 (2020) 2439–2450.
[23] L.A. Jackson, E.J. Anderson, N.G. Rouphael, P.C. Roberts, M. Makhene, R.N. Coler, M.P. McCullough, J.D. Chappell, M.R. Denison, L.J. Stevens, A.J. Pruijssers, A. McDermott, B. Flach, N.A. Doria-Rose, K.S. Corbett, K.M. Morabito, S. O'Dell, S. D. Schmidt, P.A. Swanson 2nd, M. Padilla, J.R. Mascola, K.M. Neuzil, H. Bennett, W. Sun, E. Peters, M. Makowski, J. Albert, K. Cross, W. Buchanan, R. Pikaart-Tautges, J.E. Ledgerwood, B.S. Graham, J.H. Beigel, An mRNA vaccine against SARS-CoV-2 - preliminary report, N. Engl. J. Med. 383 (2020) 1920–1931.
[24] Q. Cheng, T. Wei, L. Farbiak, L.T. Johnson, S.A. Dilliard, D.J. Siegwart, Selective organ targeting (SORT) nanoparticles for tissue-specific mRNA delivery and CRISPR-Cas gene editing, Nat. Nanotechnol. 15 (2020) 313–320.
[25] J.D. Finn, A.R. Smith, M.C. Patel, L. Shaw, M.R. Youniss, J. van Heteren, T. Dirstine, C. Ciullo, R. Lescarbeau, J. Seitzer, R.R. Shah, A. Shah, D. Ling, J. Growe, M. Pink, E. Rohde, K.M. Wood, W.E. Salomon, W.F. Harrington, C. Dombrowski, W.R. Strapps, Y. Chang, D.V. Morrissey, A single administration of CRISPR/Cas9 lipid nanoparticles achieves robust and persistent in vivo genome editing, Cell Rep. 22 (2018) 2227–2235.
[26] J. Liu, J. Chang, Y. Jiang, X. Meng, T. Sun, L. Mao, Q. Xu, M. Wang, Fast and efficient CRISPR/Cas9 genome editing in vivo enabled by bioreducible lipid and Messenger RNA nanoparticles, Adv. Mater. 31 (2019), e1902575.
[27] H. Yin, C.Q. Song, J.R. Dorkin, L.J. Zhu, Y. Li, Q. Wu, A. Park, J. Yang, S. Suresh, A. Bizhanova, A. Gupta, M.F. Bolukbasi, S. Walsh, R.L. Bogorad, G. Gao, Z. Weng, Y. Dong, V. Koteliansky, S.A. Wolfe, R. Langer, W. Xue, D.G. Anderson, Therapeutic genome editing by combined viral and non-viral delivery of CRISPR system components in vivo, Nat. Biotechnol. 34 (2016) 328–333.
[28] M. Wang, J.A. Zuris, F. Meng, H. Rees, S. Sun, P. Deng, Y. Han, X. Gao, D. Pouli, Q. Wu, I. Georgakoudi, D.R. Liu, Q. Xu, Efficient delivery of genome-editing proteins using bioreducible lipid nanoparticles, Proc. Natl. Acad. Sci. U. S. A. 113 (2016) 2868–2873.
[29] S.C. Semple, A. Akinc, J. Chen, A.P. Sandhu, B.L. Mui, C.K. Cho, D.W. Sah, D. Stebbing, E.J. Crosley, E. Yaworski, I.M. Hafez, J.R. Dorkin, J. Qin, K. Lam, K. G. Rajeev, K.F. Wong, L.B. Jeffs, L. Nechev, M.L. Eisenhardt, M. Jayaraman, M. Kazem, M.A. Maier, M. Srinivasulu, M.J. Weinstein, Q. Chen, R. Alvarez, S. A. Barros, S. De, S.K. Klimuk, T. Borland, V. Kosovrasti, W.L. Cantley, Y.K. Tam, M. Manoharan, M.A. Ciufolini, M.A. Tracy, A. de Fougerolles, I. MacLachlan, P. R. Cullis, T.D. Madden, M.J. Hope, Rational design of cationic lipids for siRNA delivery, Nat. Biotechnol. 28 (2010) 172–176.
[30] H. Zhang, S. Gao, Y. Huang, siRNA, Pharmaceutical Composition and Conjugate Which Contain siRNA, and Uses Thereof, World Intellectual Property Organization WO2016206626, 2016, pp. 1–47.
[31] K. Strebhardt, A. Ullrich, Targeting polo-like kinase 1 for cancer therapy, Nat. Rev. Canc. 6 (2006) 321–330.
[32] P. Wang, L. Zhang, W. Zheng, L. Cong, Z. Guo, Y. Xie, L. Wang, R. Tang, Q. Feng, Y. Hamada, K. Gonda, Z. Hu, X. Wu, X. Jiang, Thermo-triggered release of CRISPR-cas9 system by lipid-encapsulated gold nanoparticles for tumor therapy, Angew. Chem. Int. Ed. Engl. 57 (2018) 1491–1496.
[33] R.E. Gutteridge, M.A. Ndiaye, X. Liu, N. Ahmad, Plk1 inhibitors in cancer therapy: from laboratory to clinics, Mol. Canc. Therapeut. 15 (2016) 1427–1435.
[34] T. Yang, C. Yu, C. Wang, C. Li, M. Zhang, X. Luo, Y. Weng, A. Dong, X. Li, Y. Deng, Y. Huang, The microgravity enhanced polymer-mediated siRNA gene silence by improving cellular uptake, Biophys. Rep. 6 (2020) 266–277.
[35] D. Zhao, G. Yang, Q. Liu, W. Liu, Y. Weng, Y. Zhao, F. Qu, L. Li, Y. Huang, A photo-triggerable aptamer nanoswitch for spatiotemporal controllable siRNA delivery, Nanoscale 12 (2020) 10939–10943.
[36] C. Wang, L. Du, J. Zhou, L. Meng, Q. Cheng, C. Wang, X. Wang, D. Zhao, Y. Huang, S. Zheng, H. Cao, J. Zhang, L. Deng, Z. Liang, A. Dong, Elaboration on the distribution of hydrophobic segments in the chains of amphiphilic cationic polymers for small interfering RNA delivery, ACS Appl. Mater. Interfaces 9 (2017) 32463–32474.
[37] Z. Chen, F. Liu, Y. Chen, J. Liu, X. Wang, A.T. Chen, G. Deng, H. Zhang, J. Liu, Z. Hong, J. Zhou, Targeted delivery of CRISPR/Cas9-Mediated cancer gene therapy via liposome-templated hydrogel nanoparticles, Adv. Funct. Mater. 27 (2017).
[38] M. Jayaraman, S.M. Ansell, B.L. Mui, Y.K. Tam, J. Chen, X. Du, D. Butler, L. Eltepu, S. Matsuda, J.K. Narayanannair, K.G. Rajeev, I.M. Hafez, A. Akinc, M.A. Maier, M. A. Tracy, P.R. Cullis, T.D. Madden, M. Manoharan, M.J. Hope, Maximizing the potency of siRNA lipid nanoparticles for hepatic gene silencing in vivo, Angew Chem. Int. Ed. Engl. 51 (2012) 8529–8533.
[39] K.T. Love, K.P. Mahon, C.G. Levins, K.A. Whitehead, W. Querbes, J.R. Dorkin, J. Qin, W. Cantley, L.L. Qin, T. Racie, M. Frank-Kamenetsky, K.N. Yip, R. Alvarez, D.W. Sah, A. de Fougerolles, K. Fitzgerald, V. Koteliansky, A. Akinc, R. Langer, D. G. Anderson, Lipid-like materials for low-dose, in vivo gene silencing, Proc. Natl. Acad. Sci. U. S. A. 107 (2010) 1864–1869.
[40] F.J. Xu, Deciphering the impact of PEG antifouling layer on surface attached functional peptides in regulating cell behaviors, Chin. Chem. Lett. 30 (2019) 2051–2052.
[41] J.A. Kulkarni, D. Witzigmann, J. Leung, Y.Y.C. Tam, P.R. Cullis, On the role of helper lipids in lipid nanoparticle formulations of siRNA, Nanoscale 11 (2019) 21733–21739.
[42] R.L. Ball, K.A. Hajj, J. Vizelman, P. Bajaj, K.A. Whitehead, Lipid nanoparticle formulations for enhanced Co-delivery of siRNA and mRNA, Nano Lett. 18 (2018) 3814–3822.
[43] K.A. Whitehead, J.R. Dorkin, A.J. Vegas, P.H. Chang, O. Veiseh, J. Matthews, O. S. Fenton, Y. Zhang, K.T. Olejnik, V. Yesilyurt, D. Chen, S. Barros, B. Klebanov, T. Novobrantseva, R. Langer, D.G. Anderson, Degradable lipid nanoparticles with predictable in vivo siRNA delivery activity, Nat. Commun. 5 (2014) 4277.
[44] A. Akinc, W. Querbes, S. De, J. Qin, M. Frank-Kamenetsky, K.N. Jayaprakash, M. Jayaraman, K.G. Rajeev, W.L. Cantley, J.R. Dorkin, J.S. Butler, L. Qin, T. Racie, A. Sprague, E. Fava, A. Zeigerer, M.J. Hope, M. Zerial, D.W. Sah, K. Fitzgerald, M. A. Tracy, M. Manoharan, V. Koteliansky, A. Fougerolles, M.A. Maier, Targeted delivery of RNAi therapeutics with endogenous and exogenous ligand-based mechanisms, Mol. Ther. 18 (2010) 1357–1364.
[45] S.F. Dowdy, Overcoming cellular barriers for RNA therapeutics, Nat. Biotechnol. 35 (2017) 222–229.
[46] C. Li, J. Zhou, Y. Wu, Y. Dong, L. Du, T. Yang, Y. Wang, S. Guo, M. Zhang, A. Hussain, H. Xiao, Y. Weng, Y. Huang, X. Wang, Z. Liang, H. Cao, Y. Zhao, X.-J. Liang, A. Dong, Y. Huang, Core role of hydrophobic Core of polymeric nanomicelle in endosomal escape of siRNA, Nano Lett. 21 (2021) 3680–3689.
[47] A. Wittrup, J. Lieberman, Knocking down disease: a progress report on siRNA therapeutics, Nat. Rev. Genet. 16 (2015) 543–552.
[48] J. Gilleron, W. Querbes, A. Zeigerer, A. Borodovsky, G. Marsico, U. Schubert, K. Manygoats, S. Seifert, C. Andree, M. Stoter, H. Epstein-Barash, L. Zhang, V. Koteliansky, K. Fitzgerald, E. Fava, M. Bickle, Y. Kalaidzidis, A. Akinc, M. Maier, M. Zerial, Image-based analysis of lipid nanoparticle-mediated siRNA delivery,

intracellular trafficking and endosomal escape, Nat. Biotechnol. 31 (2013) 638–646.
[49] H.C. Kang, Y.H. Bae, pH-tunable endosomolytic oligomers for enhanced nucleic acid delivery, Adv. Funct. Mater. 17 (2007) 1263–1272.
[50] I. El Dika, H.Y. Lim, W.P. Yong, C.C. Lin, J.H. Yoon, M. Modiano, B. Freilich, H. J. Choi, T.Y. Chao, R.K. Kelley, J. Brown, J. Knox, B.Y. Ryoo, T. Yau, G.K. Abou-Alfa, An open-label, Multicenter, phase I, dose escalation study with phase II expansion cohort to determine the safety, pharmacokinetics, and preliminary antitumor activity of intravenous TKM-080301 in subjects with advanced hepatocellular carcinoma, Oncol. 24 (2019), 747-e218.